Available online at www.sciencedirect.com
SCIENCE DIRECT®
Journal of the European Ceramic Society 25 (2005) 1991–1995
www.elsevier.com/locate/jeurceramsoc

Characterization of perovskite powders for cathode and oxygen membranes made by different synthesis routes

J. Sfeir [a,*], S. Vaucher [b], P. Holtappels [c], U. Vogt [c], H.-J. Schindler [c], J. Van herle [d], E. Suvorova [e], P. Buffat [e], D. Perret [d], N. Xanthopoulos [f], O. Bucheli [a]

[a] *HTceramix SA, EPFL, PSE-A, CH-1015 Lausanne, Switzerland*
[b] *Swiss Federal Laboratories for Materials Testing and Research, EMPA, Feuerwerkstrasse 39, CH-3602 Thun, Switzerland*
[c] *Swiss Federal Laboratories for Materials Testing and Research, EMPA, Ueberlandstrasse 129, CH-8600 Dübendorf, Switzerland*
[d] *Swiss Federal Institute of Technology Lausanne, EPFL, STI-ISE-LENI, CH-1015 Lausanne, Switzerland*
[e] *Swiss Federal Institute of Technology Lausanne, EPFL, SB-CIME, CH-1015 Lausanne, Switzerland*
[f] *Swiss Federal Institute of Technology Lausanne, EPFL, STI-IMX-LMCH, CH-1015 Lausanne, Switzerland*

Available online 31 March 2005

Abstract

Strontium lanthanum manganite (LSM) and lanthanum ferrite (LSF) perovskite cathode and oxygen membrane materials were synthesized using different techniques: spray pyrolysis, a modified citrate route, oxalate and carbonate co-precipitations. The use of Ca, a cheaper substituent on the *A*-site, was explored along to the substitution of La by Pr. The differently sourced powders were characterized by TG/DTA, XRD, ICP, TEM, XPS, PSD and BET. The co-precipitation of La, Ca and Fe was also possible using the cyanide route. This complexation method allowed the precipitation of a crystalline phase as evidenced by XRD. Among all methods, the cyanide and carbonate co-precipitation allowed the lowest perovskite phase transformation for LSF and LCF, followed by the nitrate (i.e. '*spray pyrolysis*'). These phase transformation differences affected much the particle size distribution and the surface areas of these materials, the carbonate and the cyanide routes giving rise to very fine powders in the nm range. XPS and TEM analyses indicated uneven composition distributions. These different powder characteristics are expected to affect the catalytic and electrochemical properties of these materials.

Keywords: Powders-chemical preparation; Electron microscopy; Perovskites; Fuel cells; Membranes

1. Introduction

The lanthanide transition-metal oxides are of technological importance for their use in solid oxide fuel cell, catalysis, oxygen membrane reactors and sensors.[1–5] In SOFC, strontium substituted lanthanum manganite (LSM) is commonly used as a high temperature cathode material. Strontium substituted lanthanum ferrite (LSF) is investigated as alternative cathode material in medium temperature SOFCs but also as potential oxygen membrane for oxygen and syngas production. These materials are commonly investigated in relation to their electronic, catalytic and electrochemical properties.

Preparation conditions are in many cases responsible for structural differences and thus for the disparity in catalytic,[6] electrocatalytic and electrochemical properties of oxides. In this study, we investigate the influence of different fabrication procedures on the final microstructure and composition of these materials for their use as SOFC cathodes or oxygen membrane materials. Calcination conditions, composition homogeneity, phase purity, powder size distribution and the ease of fabrication are considered.

2. Experimental

The different perovskite powders were prepared according to the formula $(La_{1-x}A_x)_yMO_{3-\delta}$ with A = Ca or Sr, and M = Mn or Fe. All chemicals were purchased from Fluka and the precursors were taken from the same batch.

* Corresponding author. Present address: Swiss Federal Laboratories for Materials Testing and Research, EMPA, Ueberlandstrasse 129, CH-8600 Dübendorf, Switzerland. Tel.: +41 76 4155905.
E-mail address: joseph.sfeir@empa.ch (J. Sfeir).

0955-2219/$ – see front matter © 2005 Elsevier Ltd. All rights reserved.
doi:10.1016/j.jeurceramsoc.2005.03.124

The spray pyrolysis synthesis was made following Ref. [7]. The powders thus obtained were homogenized by ball-milling and then calcined at 1450 °C for 2 h. Subsequently, further processing steps (ball-milling for 150 h and sieving) were added to obtain the desired powder characteristics.

Citrate gelling was made following the procedure presented by Douy.[8] The ligand (L) concentration was set to 1 M and adjusted to $M^{n+}L_n$ (M^{n+}, reacting metal).

For oxalate precipitation, the procedure optimized by Van herle et al.[9] for the fabrication of ceria-based powders was implemented. The optimal precipitation conditions were identified as: pH ≈ 7, $[M^{n+}] = 1$ M, [L] = 0.5 M. Some leaching was observed for Fe and Mn, independently of the conditions.

The carbonate precipitations were obtained following a modified route using $(NH_4)_2CO_3$.[10,11] The optimal conditions were identified as: natural pH ≈ 8, $[M^{n+}] = 3$–1 M, [L] = 0.5–1 M. No Fe leaching was observed (no coloration upon KSCN addition).

For the cyanide route, potassium $[Fe^{II}(CN)_6]^{4-}$ and $[Fe^{III}(CN)_6]^{3-}$ were used as precipitating agents, based on experiments made by Vaucher et al.[12,13] on Co and Cr. The metals concentration was set to 3 M. Sr substituted $LaFeO_3$ could not be synthesized as Sr did not precipitate as observed by cross reactions between Sr nitrate and $[Fe^{II}(CN)_6]^{4-}$ or $[Fe^{III}(CN)_6]^{3-}$. For Ca, precipitation was only observed with $[Fe^{II}(CN)_6]^{4-}$. Thus, Ca-substituted $LaFeO_3$ was the only powder produced following this procedure. Interestingly, to our knowledge, this is the first reported cyanide precipitation relating La, Ca and Fe, as previous works in this field are based on the binary $LaFeO_3$, with $[Fe^{III}(CN)_6]^{3-}$ as precursor.[14,15] The results will be reported in more details elsewhere.

A summary of the different powders is given in Table 1. All the precipitates were subsequently washed with the solvent followed by isopropanol. Final calcination temperatures were varied. The powders thus obtained were characterized by TG/DTA, XRD, TEM-EDS, XPS, BET, PSD and ICP.

Electrochemical tests were made following the same procedure described elsewhere.[5] Organic pastes of three differently sourced LSF powders with the same nominal composition were applied as SOFC cathodes on anode supported cells. Tests were made at 800 °C in H_2/air.

3. Results and discussion

3.1. Powder characterization

From TG/DTA analyses on precipitates, the carbonates were observed to allow first the perovskite transformation at a temperature of 650 °C. The observed trend was as follows:

$$LSF_{carbonate}650\,^{\circ}C < LSF_{nitrate}660\,^{\circ}C < LSF_{citrate} 680\,^{\circ}C < LSF_{axalate}800\,^{\circ}C$$

$$LCF_{carbonate}650\,^{\circ}C < LCF_{cyanide}670\,^{\circ}C < LCF_{axalate} 700\,^{\circ}C < LCF_{citrate}900\,^{\circ}C$$

All decompositions were observed to proceed concomitantly, with a temperature close to that of the La complex. For the carbonate precipitates containing Fe, the iron moiety is thought to exist as a hydroxy rather than a carboxy group as no Fe^{III} carbonate could be found in literature.

All co-precipitated powders were amorphous before calcination, except for the LCF precursor made by the cyanide route, in which the precipitation of a nanocrystalline hexacyano complexe occurred. XRD analyses were also performed on powders calcined at different temperatures, mainly at 900, 1000 and 1100 °C. In the case of oxalate powders, XRD-phase purity was only reached after sintering at 1100 °C. This was also the case for the LCF and LSM obtained from carbonates. For the cyanide, a phase trans-

Table 1
Summary of the ICP analyses

ICP analysis		Experimental composition						Sum	Nominal sum	% Deviation
Label	Nominal composition	La	Sr	Mn	Fe	Ca	Pr			
5ULSM73-P	$(La_{0.7}Sr_{0.3})_{0.95}MnO_{3-\delta}$	0.678	0.288	1	0.03	0	0.02	1.966	1.95	100.8
LSF55-P	$La_{0.5}Sr_{0.5}FeO_{3-\delta}$	0.537	0.507	–	1	–	–	2.044	2	102.2
5ULSF73-P	$(La_{0.7}Sr_{0.3})_{0.95}FeO_{3-\delta}$	0.733	0.312	0	1	0	0.02	2.045	1.95	104.9
5ULCF73-P	$(La_{0.7}Ca_{0.3})_{0.95}FeO_{3-\delta}$	0.875	0.01	0.01	1	0.252	0.02	2.127	1.95	109.1
5UPCF73-P	$(Pr_{0.7}Ca_{0.3})_{0.95}FeO_{3-\delta}$	0.01	0	0	1	0.287	0.828	2.115	1.95	108.5
3ULSM$\frac{2}{3}\frac{1}{3}$-Ci	$(La_{0.75}Sr_{0.25})_{0.97}MnO_{3-\delta}$	0.731	0.255	1	–	–	–	1.986	1.97	100.8
5ULSF73-Ci	$(La_{0.7}Sr_{0.3})_{0.95}FeO_{3-\delta}$	0.685	0.277	0	1	0	0.01	1.962	1.95	100.6
LSF37-Ca	$La_{0.3}Sr_{0.7}\ FeO_{3-\delta}$	0.3	0.672	–	1	–	–	1.972	2	98.6
LSF55-Ca	$La_{0.5}Sr_{0.5}FeO_{3-\delta}$	0.505	0.494	–	1	–	–	1.999	2	99.95
5ULSF73-Ca	$(La_{0.7}Sr_{0.3})_{0.95}FeO_{3-\delta}$	0.704	0.283	0	1	0	0.01	1.987	1.95	101.9
LSF73-Ca	$La_{0.7}Sr_{0.3}FeO_{3-\delta}$	0.713	0.295	1	–	–	–	2.008	2	100.4
5OLSF73-Ca	$(La_{0.7}Sr_{0.3})_{1.05}FeO_{3-\delta}$	0.757	0.314	1	–	–	–	2.071	2.05	101.0
5UPSF73-Ca	$(Pr_{0.7}Sr_{0.3})_{0.95}FeO_{3-\delta}$	–	0.278	1	–	–	0.851	2.129	1.95	109.2

The prefix and suffix stand for: U, under-stoichiometric; O, over-stoichiometric; P, '*spray pyrolysis*'; Ci, citrate; Ca, carbonate. The error on Fe detection is of about 0.03.

formation to the perovskite structure is observed at 450 °C in which the cyanide ligands in the hexacyano-precipitate are replaced by oxygen. For the $La_{1-x}Sr_xFeO_3$ made from carbonates, XRD-phase purity was already reached at 800 °C in contrast to '*spray pyrolysis*' where higher thermal treatments (1200 °C) were needed.

ICP elemental composition analyses (Table 1) indicated that all powders were, within a max of 4%, near the nominal values with the exception of the Pr perovskites (probably due to uncertainty in the Pr precursor content).

TEM-EDS measurements were done on a dozen of particles of 10–200 nm. Preliminary analysis shows large scattering in the Sr or Ca content among these particles. For 5ULSM73-P, the generic formula was $La_{1-x}Sr_xMnO_m$, with $0.02 \leq x \leq 0.44$. For 5ULSF73-P, the Sr content varied with $0.04 \leq x \leq 0.24$. With 5ULCF73-P, the EDS analysis suggests the generic formula $(La_{1-x}Ca_x)_{0.54}Fe_{0.46}O_m$, with $0.1 \leq x \leq 0.3$. For the 5ULSF73-Ci, an estimated $(La + Sr)_7Fe_3O_m$ formula was obtained. The Sr content varied as $0.01 \leq x \leq 0.36$. From diffraction patterns many phases were present. For the phases containing the three metal elements, $La_2SrFe_2O_7$ and $(La_{1-x}Sr_x)FeO_3$, identified the closest this composition. In the case of 5ULSF73-Ca a generic formula of $(La_{1-x}Sr_x)FeO_m$ with $0.16 \leq x \leq 0.34$ was obtained and the powder corresponded well to the $LaFeO_3$ phase with different Sr content. 5UPCF73-P contained multiple phases. By EDS and diffraction, some areas indicated the presence of a Pr rich oxide, lacking Fe and Ca, and related to the $Pr_2O_{7,\ trigonal}$ phase. The generic formula obtained was $Pr_{1-x}Ca_xFeO_m$, with $0.04 \leq x \leq 0.24$.

In all these cases, the nominal value for x would have been of 0.285. These nano-scale discrepancies occur independently of the fabrication route and the XRD purity. Statistical analyses would be needed to confirm these results but also to get a clear idea on the scattering caused by the different methods. This work is on-going. Globally, from this qualitative analysis, 5ULSF73-Ca is observed to show a more homogeneous Sr distribution than in the cases of 5ULSF73-Ci and 5ULSF73-P.

Furthermore, XPS measurements showed differential segregation on the surface of these powders with a much higher ratio for the *A*-site elements (Table 2). Such a high *A*-site concentration is also observed on other perovskite powders[3,16,17] and is thought to influence the catalytic activities due to differences in the number of active reaction sites. Among all powders, a much higher Sr content was observed for 5ULSF73-Ci and 3ULSM$\frac{2}{3}\frac{1}{3}$-Ci.

PSD and BET analyses (Table 2) made on some of the samples show that citrate powders had much coarser particles probably due to the short milling step (24 h). Coarse '*spray pyrolysis*' powders sintered at 1400 °C was brought to a much finer structure upon intensive milling (≈150 h). 5ULSF73-P shows a large surface area indicating the presence of mesoporous agglomerates. LSF-carbonates, on the other hand, showed the finest structure after sintering at 900 °C.

Globally, these results indicate the possible implementation of carbonate co-precipitation as an alternative method for the synthesis of LSM and LSF on a large scale. A preliminary study made on a semi-pilot installation using static mixers and pumps showed the feasibility of this approach. A few hundreds of grams were produced easily in 5 min time.

3.2. Influence of the fabrication route on the electrochemical performance

Preliminary electrochemical measurements made at 800 °C on 5ULSF73-Ci, 5ULSF73-Ca and 5ULSF73-P based cathodes having the same nominal composition presented discrepancies in their behaviour (Fig. 1). The 5ULSF73-Ci cathode performed poorly when compared to the other two.

These results might be understood in light of the disparities in the morphology (PSD and BET) and/or powder characteristics (TEM, XPS and ICP) reported above. Electrochemical simulations predict a significant enhancement of performance for well-structured mixed ionic-electronic cathodes.[18] The geometry dependence of the polarization resistance is considerably influenced by the ratio k/D. This value is of about 30–270 for LSF and 10^5 to 10^6 for LSM.[19,20] The nanostructured 5ULSF73-Ca and 5ULSF73-P (PSD, 100–500 nm) performed much better than the coarse 5ULSF73-Ci (PSD, 1–2 μm), in agreement with the model. The outer layer composition of the powders might also influence the cathode performance, as the surface is the site of the

Table 2
Summary of the XPS surface analyses given in percent and of the PSD and BET values

Powder	XPS ratio							XPS composition	PSD (μm)	BET (m^2/g)
	Mn/La+Sr	Fe/La+Sr	Fe/La+Ca	Fe/Pr+Ca	La/Sr	La/Ca	Pr/Ca			
5ULSM73-P	38/62				71/29			$(La_{0.71}Sr_{0.29})_{0.62}Mn_{0.38}$	0.387	
5ULSF73-P		32/68			70/30			$(La_{0.70}Sr_{0.30})_{0.68}Fe_{0.32}$	0.504	15.4
5ULCF73-P			31/69			71/29		$(La_{0.69}Ca_{0.31})_{0.71}Fe_{0.31}$	0.459	
5UPCF73-P				25/75			74/26	$(Pr_{0.74}Ca_{026})_{0.75}Fe_{0.25}$	–	–
5ULSF73-Ci		45/56			57/44			$(La_{0.57}Sr_{0.44})_{0.68}Fe_{0.32}$	1–2	3.82
3ULSM$\frac{2}{3}\frac{1}{3}$-Ci	–				–			–	1–2	3.73
5ULSF73-Ca		36/64			63/37			$(La_{0.63}Sr_{0.37})_{0.64}Fe_{0.36}$	0.1	8.04

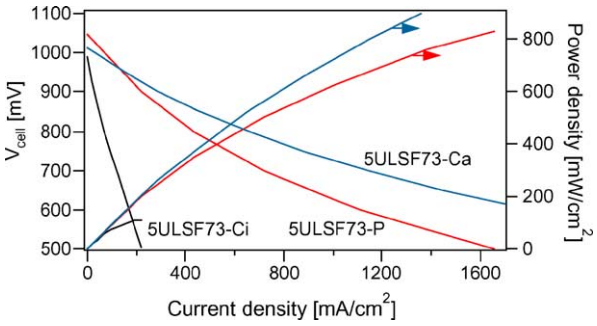

Fig. 1. Electrochemical characterization at 800 °C of 5ULSF73-P, 5ULSF73-Ci and 5ULSF73-Ca SOFC cathodes deposited on a thin anode supported electrolyte and sintered at 1100 °C/4 h. The electrolyte thickness was of 5 μm. The cathode and the cell areas were of 1 cm^2 and 16 cm^2, respectively. Air and wet H_2 were used at the cathode and anode, respectively.

oxygen reduction reaction. These considerations are also true for oxygen membrane materials.[21] However, further studies are needed to clarify these dependencies.

4. Conclusions

Strontium lanthanum manganite and ferrite were produced by different techniques: '*spray pyrolysis*', a modified citrate route, oxalate, carbonate and cyanide co-precipitation. The influence of the different fabrication procedures on the final microstructure and composition of these materials were investigated. Powders were characterized by TG/DTA, XRD, ICP, TEM, XPS, PSD and BET.

'*Spray pyrolysis*' produced mesoporous agglomerates after intensive ball-milling. Powders with a $d_{50} = 500$ nm were thus obtained.

The carbonate route was observed to deliver a finer powder with a more homogeneous composition (100 nm, TEM). These results indicate the possible implementation of carbonate co-precipitation as an alternative route for the synthesis of lanthanide ferrite and manganite. A semi-pilot installation made using static mixers showed the feasibility of this approach.

The co-precipitation of La, Ca and Fe was also possible using the cyanide route giving rise to a crystalline complex. This is to our knowledge the first reported cyanide precipitation relating La, Ca, and Fe using $[Fe^{II}(CN)_6]^{4-}$.

ICP analyses on all samples showed slight fluctuations between the differently sourced powders. However, due to distinct synthesis routes, sintering temperatures and processing steps morphological differences were observed (TEM, XPS, BET and PSD).

As expected, the microstructure and surface composition of these powders triggered disparities in their electrochemical response (SOFC cathode tests). The relative importance of each of these properties is not very clear yet.

Acknowledgement

This work was financed under the TNS 5991.1/6555.1 contract by the Swiss Confederation.

References

1. Gellings, P. J. and Bouwmeester, H. J. M., Solid state aspects of oxidation catalysis. *Catal. Today*, 2000, **58**, 1–53.
2. Gellings, P. J. and Bouwmeester, H. J. M., Ion and mixed conducting oxides as catalysts. *Catal. Today*, 1992, **12**, 1–105.
3. Sfeir, J., Buffat, P., Möckli, P., Xanthopoulos, N., Vasquez, R., Mathieu, H. J., Van herle, J. and Thampi, K. R., Lanthanum chromite based catalysts for oxidation of methane directly on SOFC anodes. *J. Catal.*, 2001, **202**, 229–244.
4. Middleton, H., Diethelm, S., Ihringer, R., Larrain, D., Sfeir, J. and Van herle, J., Co-casting and co-sintering of porous MgO support plates with thin dense perovskite layers of $LaSrFeCoO_3$. *J. European Ceram. Soc.*, 2004, **24**, 1083–1086.
5. Sfeir, J., Van herle, J. and Vasquez, R., $LaCrO_3$-based anodes for methane oxidation. In *Fifth European Solid Oxide Fuel Cell Forum*, ed. J. Huijsmans, 2002, pp. 570–577.
6. Bell, R. J., Millar, G. J. and Drennan, J., Influence of synthesis route on the catalytic properties of $La_{1-x}Sr_xMnO_3$. *Solid State Ion.*, 2000, **131**, 211–220.
7. Holtappels, P., Vogt, U., Schindler, H. and Gut, B., Perovskite Synthesis by Spray Pyrolysis. In *Fifth European Solid Oxide Fuel Cell Forum*, ed. J. Huijsmans. Lucerne, Switzerland, 2002, pp. 103–107.
8. Douy, A., Polyacrylamide gel: an efficient tool for easy synthesis of multicomponent oxide precursors of ceramics and glasses. *Int. J. Inorgan. Mater.*, 2001, **3**, 699–707.
9. Van herle, J., Horita, T., Kawada, T., Sakai, N., Yokokawa, H. and Dokiya, M., Sintering behaviour and ionic conductivity of yttria-doped ceria. *J. European Ceram. Soc.*, 1996, **16**, 961–973.
10. Li, G.-J., Huang, X.-X., Guo, J.-K. and Chen, D.-M., Ni-coated Al_2O_3 powders. *Ceram. Int.*, 2002, **28**, 623–626.
11. Tanaka, J., Takahashi, K., Yajima, Y. and Tsukioka, M., Lattice constants of monoclinic $(La_{0.8}Ca_{0.2})MnO_3$. *Chem. Lett.*, 1982, 1847–1850.
12. Vaucher, S., Dujardin, E., Lebeau, B., Hall, S. and Mann, S., Higher order construction of molecule-based magnets. *Chem. Mater.*, 2001, **13**, 4408–4410.
13. Vaucher, S., Fielden, J., Li, M., Dujardin, E. and Mann, S., Molecule-based magnetic nanoparticles: synthesis of cobalt hexacyanoferrate, cobalt pentacyanonitrosylferrate, and chromium hexacyanochromate coordination polymer in water-in-oil microemulsions. *Nano Lett.*, 2002, **2**, 225–229.
14. Sadaoka, Y., Traversa, E., Nunziante, P. and Sakamoto, M., Preperation of perovskite-type $LaFe_xCo_{1-x}O_3$ by thermal decomposition of heteronuclear complex, $LaFe_xCo_{1-x}(CN)_6]\cdot n$H2O for electroceramic applications. *J. Alloys Compounds*, 1997, **261**, 182–186.
15. Hulliger, F., Landolt, M. and Vetsch, H., Rare-earth ferricyanides and chromicyanides $LnT(CN)_6\cdot nH_2O$. *J. Solid State Chem.*, 1976, **18**, 283–291.
16. Gunasekaran, N., Bakshi, N., Alcock, C. B. and Carberry, J. J., Surface characterization and catalytic properties of perovskite type solid oxide solutions, $La_{0.8}Sr_{0.2}BO_3$ (B=Cr, Mn, Co or Y). *Solid State Ion.*, 1996, **83**, 145–150.
17. Tabata, K., Matsumoto, I. and Kohiki, S., Surface characterization and catalytic properties of $La_{1-x}Sr_xCoO_3$. *J. Mater. Sci.*, 1987, **22**, 1882–1886.

18. Fleig, J. and Maier, J., The polarization of mixed conducting SOFC cathodes: effects of surface reaction coefficient, ionic conductivity and geometry. *J. European Ceram. Soc.*, 2004, **24**, 1343–1347.
19. Ishigaki, T., Yamauchi, S., Kishio, K., Mizusaki, J. and Fueki, K., Diffusion of oxide ion vacancies in perovskite-type oxides. *J. Solid State Chem.*, 1988, **73**, 179–187.
20. Adler, S. B., Lane, J. A. and Steele, B. C. H., Electrode kinetics of porous mixed-conducting oxygen electrodes. *J. Electrochem. Soc.*, 1996, **143**, 3554–3564.
21. Diethelm, S., Van herle, J., Sfeir, J. and Buffat, P., Influence of microstructure on oxygen transport in perovskite type membranes. *British Ceram. Trans.*, 2004, **103**, 147–152.